

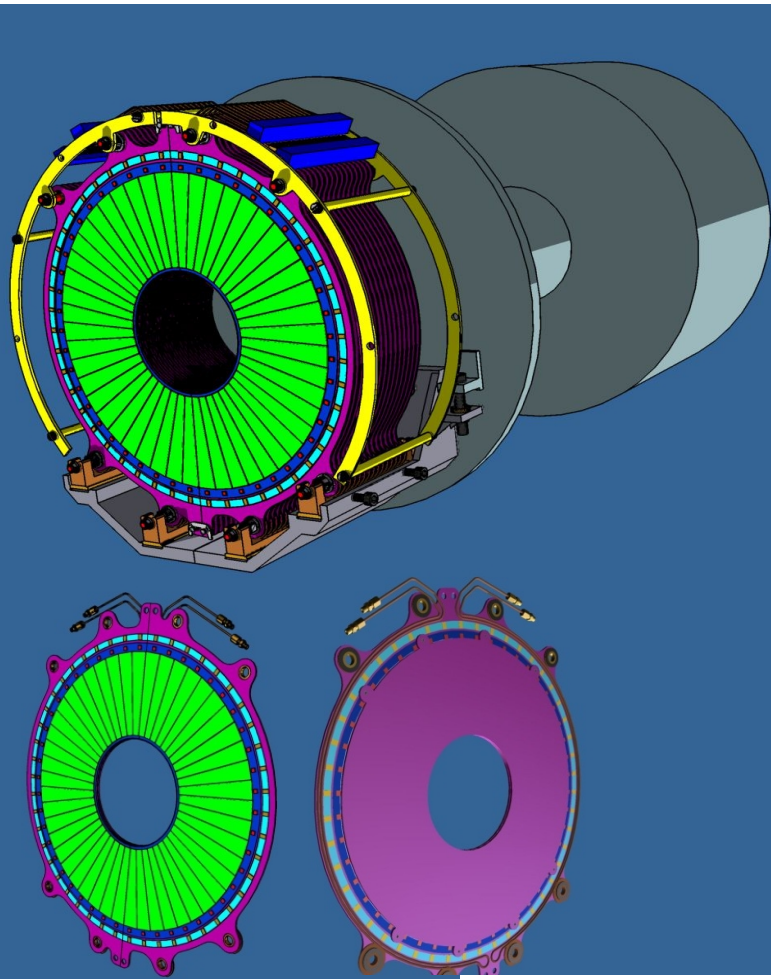
## Hamamatsu Silicon Sensors

Arkadiusz Moszczynski, Wojciech Wierba, Krzysztof Oliwa, Eryk Kielar,  
Leszek Zawiejski, Institute of Nuclear Physics PAN  
Marek Idzik, University of Science and Technology AGH

- Laboratories
- Sensors characteristics

# LumiCal calorimeter - toward the prototype

The current ( up to April 2009) design:  
before ILD integration meeting at Paris in June



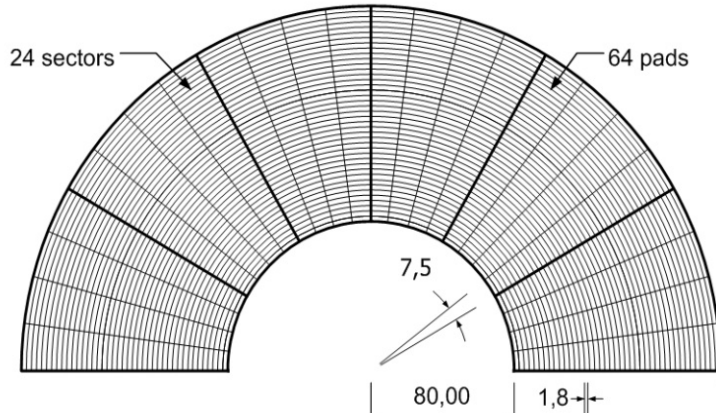
EM Si/W calorimeter with 30 layers  
with the following thicknesses:

Tungsten	- 3.5 mm
Silicon sensor	- 0.32 mm
Support	- 0.6 mm
Electronic space	- 0.1 mm
Inner radius of the active area	- 80 mm
Outer radius	- 195 mm
Sensor segmentation –	
64 cylinders with 48 sectors in azimuth	
Calorimeter can be placed	2270 mm from IP

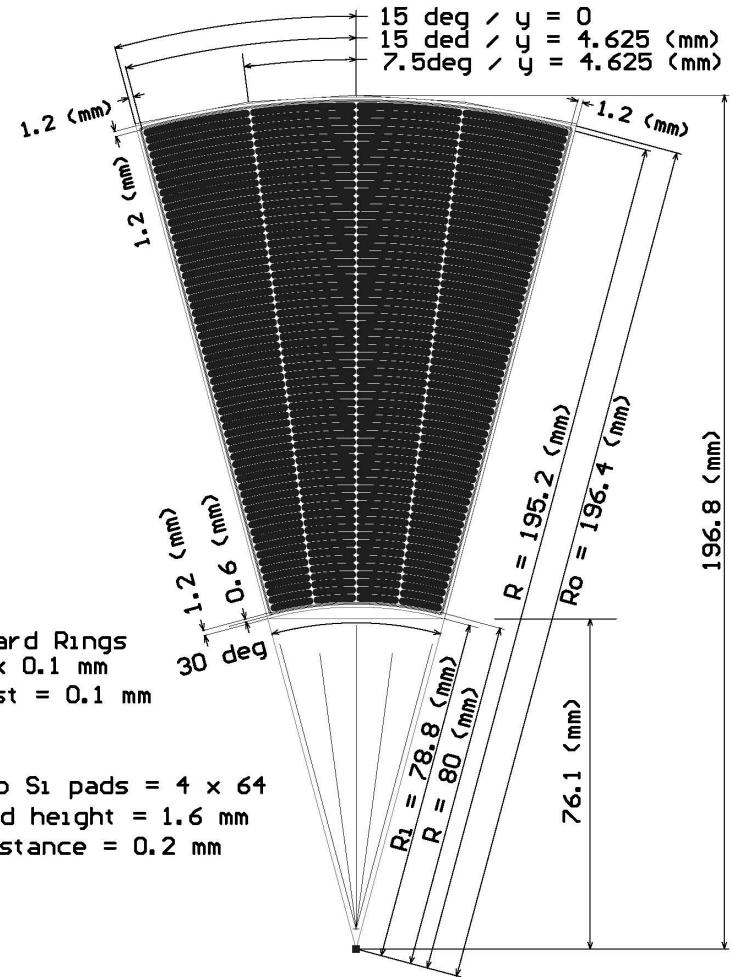
Angular coverage (silicon detectors) from ~ 32 mrad to 76 mrad  
(for ILD installation place)

# Silicon sensors - design

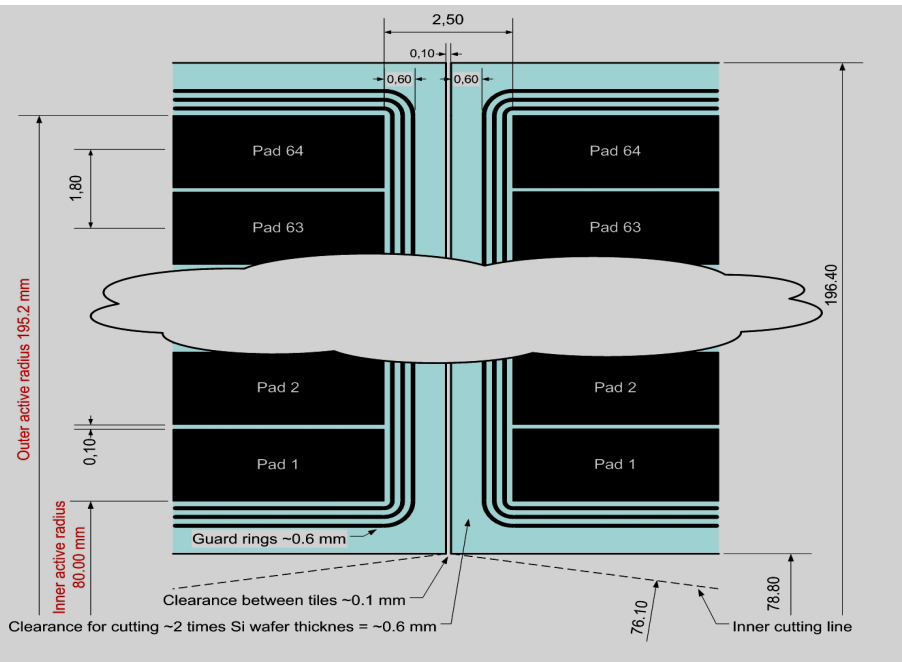
## Silicon sensor half plane



## Top Layer & Dimensions



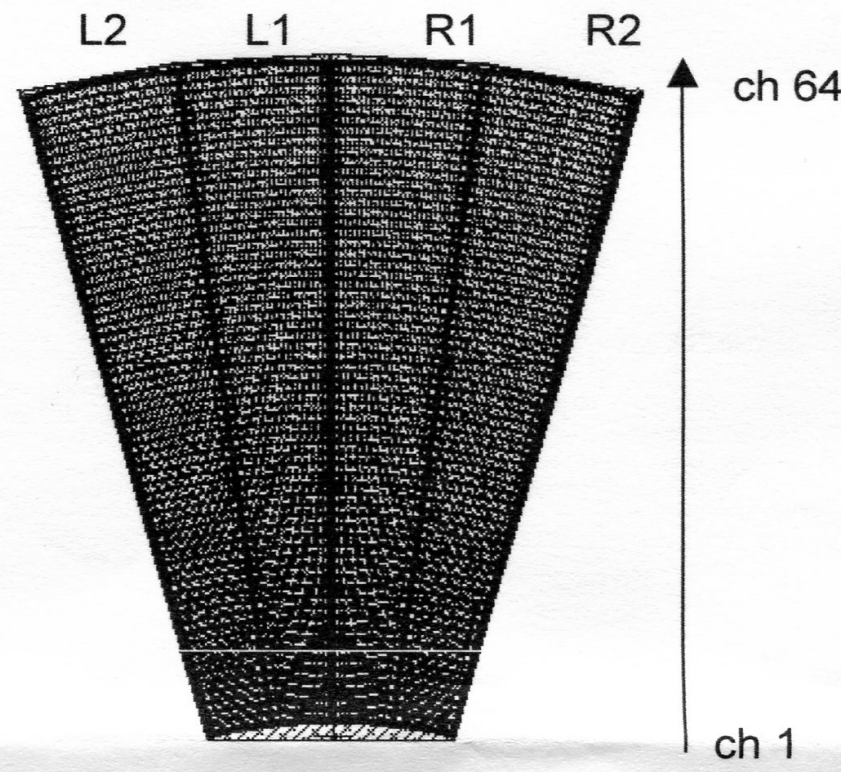
Segmentation of 4 sectors produced by Hamamatsu



Details of the structure: gap between tiles

# Hamamatsu sensors - pad number description

chipNo.	Number of NGCh	NGch
25	0	
26	1	L2-49 Leaky
27	0	
29	0	
36	1	L1-29 Leaky
42	1	L1-29 Leaky
50	0	
51	0	
52	0	
53	0	
55	0	
56	0	
57	0	
58	0	
59	0	
60	0	
61	0	
62	0	
63	1	L2-44 Leaky
64	0	



Basic sensors parameters:  
 N-type silicon, p<sup>+</sup> strips, n<sup>+</sup> backplane  
 Crystal orientation <100>  
 320 μm thickness ± 15 μm  
 Strip pitch 1.8 mm  
 Strip p<sup>+</sup> width 1.6 mm  
 Strip Al metallization width 1.7 mm

# IFJ PAN Laboratory - probe station for visual inspection



The device is used  
For visual inspection only.

The installed  
in microscope camera  
allows  
to receive picture of the  
Investigated sensor on  
the monitor screen.

Electrical movable table  
supplied  
a X,Y movements  
in steps of  $1\ \mu\text{m}$   $\rightarrow$   
inspection of the details  
of the sensor structure

Alessi probe station used for visual inspection of Hamamatsu detectors

# UST- AGH - probe station for electrical measurements C-V, I-V



Device has „black box” – measurements in darkness.

To check measurements, two different methods were used:  
with GPIB (General Purpose Interface Bus) for automatic transfer data between device and computer and old style HP instrument

Alessi probe station used for electrical measurements on Hamamatsu detectors

# IFJ PAN Lab - visual inspection



Fragment of boundary region between guard-ring and pad. The difference between dimensions of metallization outstanding over  $p^+$  implants can be clearly seen.

# IFJ PAN Lab - visual inspection



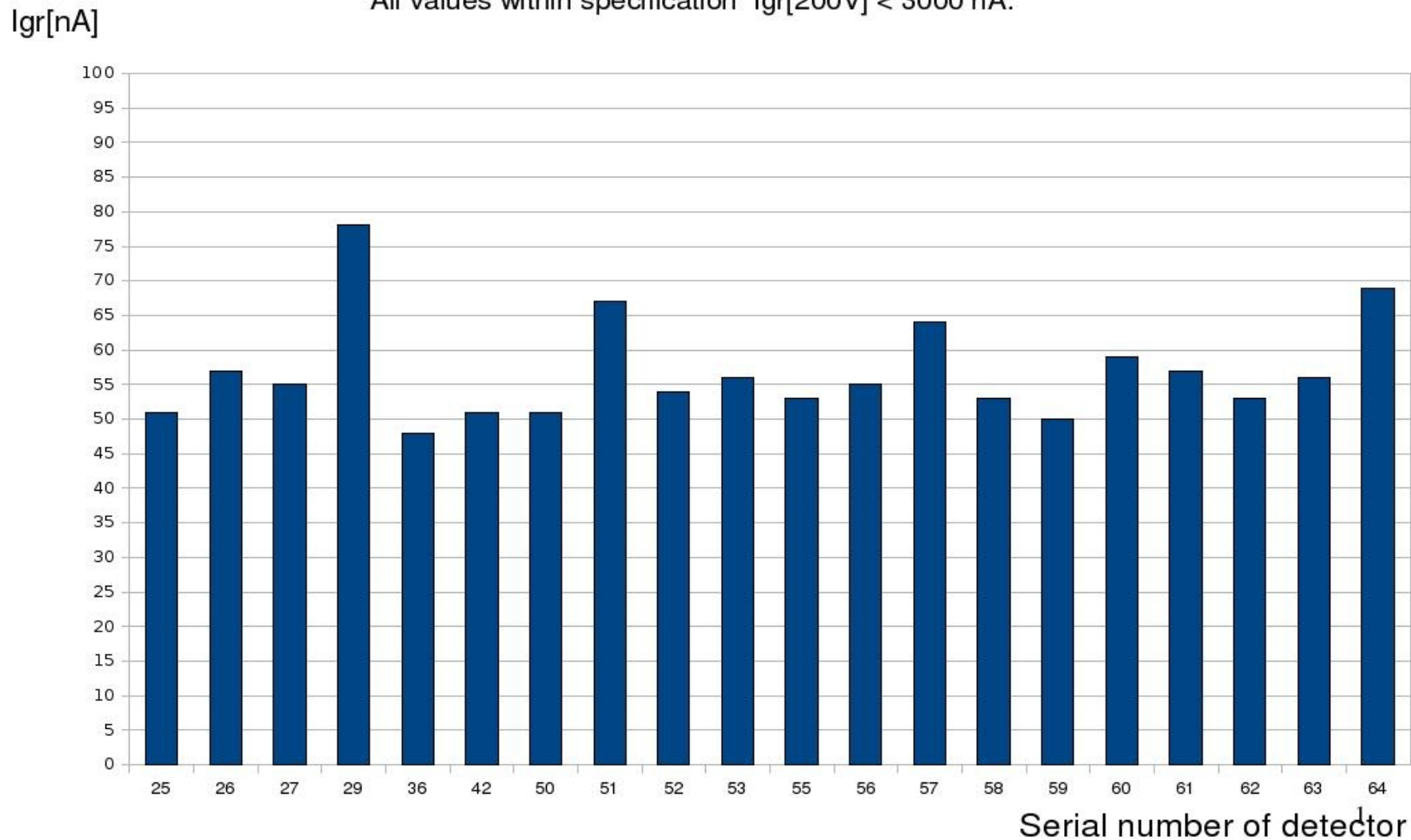
The corner fragment of guard-rings system



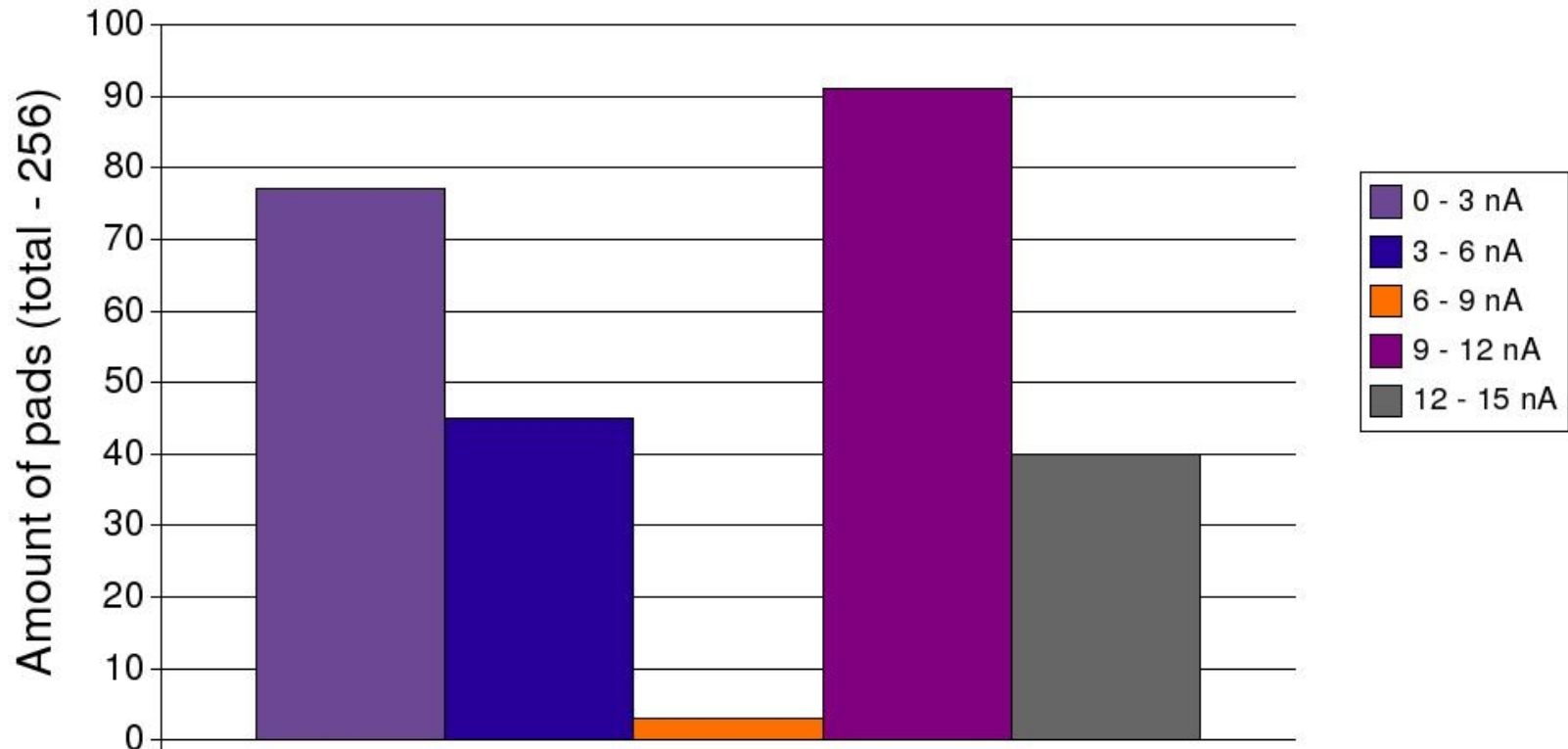
# Hamamats original measurements – guard-ring currents

Values of  $I_{gr}$  [200V] at most inner guard ring, taken from Hamamatsu data sheet.

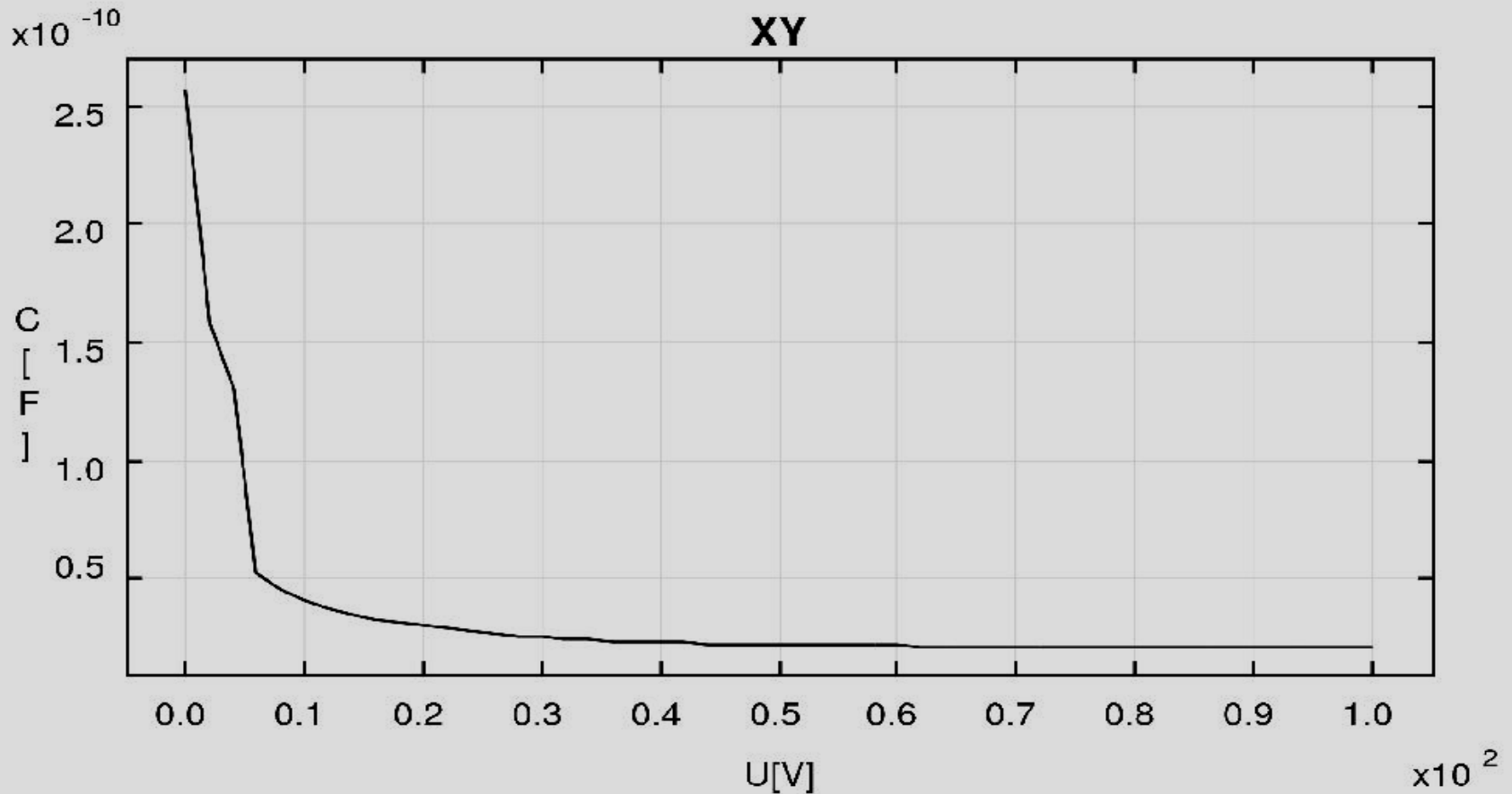
All values within specification  $I_{gr}[200V] < 3000$  nA.



Distribution of  $I_{pad}[200V]$  on Hamamatsu detector No. 25  
Taken from Hamamatsu test data sheet



# Pad measurement : capacitance - voltage plot

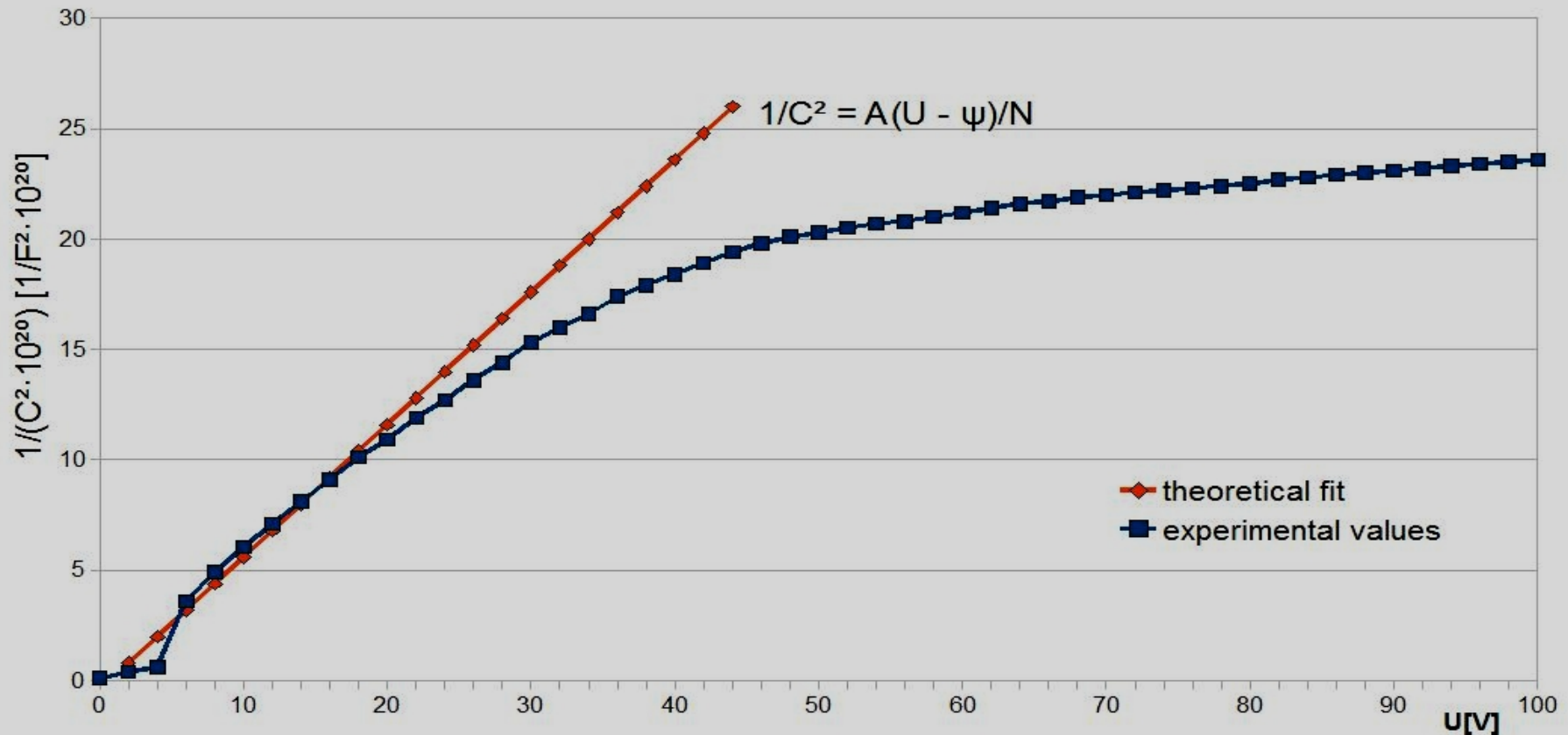


## Typical example of C-V measurements on Hamamatsu detectors.

The measurement in figure was taken on pad L263 of detector 25.

Signal frequency  $f = 1\text{MHz}$ , signal amplitude  $U_m = 100\text{mV}$ , step = 2V.

Pad measurement : C-V plot transformed to  $1/C^2 - V$  plot  
Estimation: depletion voltage, donor concentration in Si -> resistivity



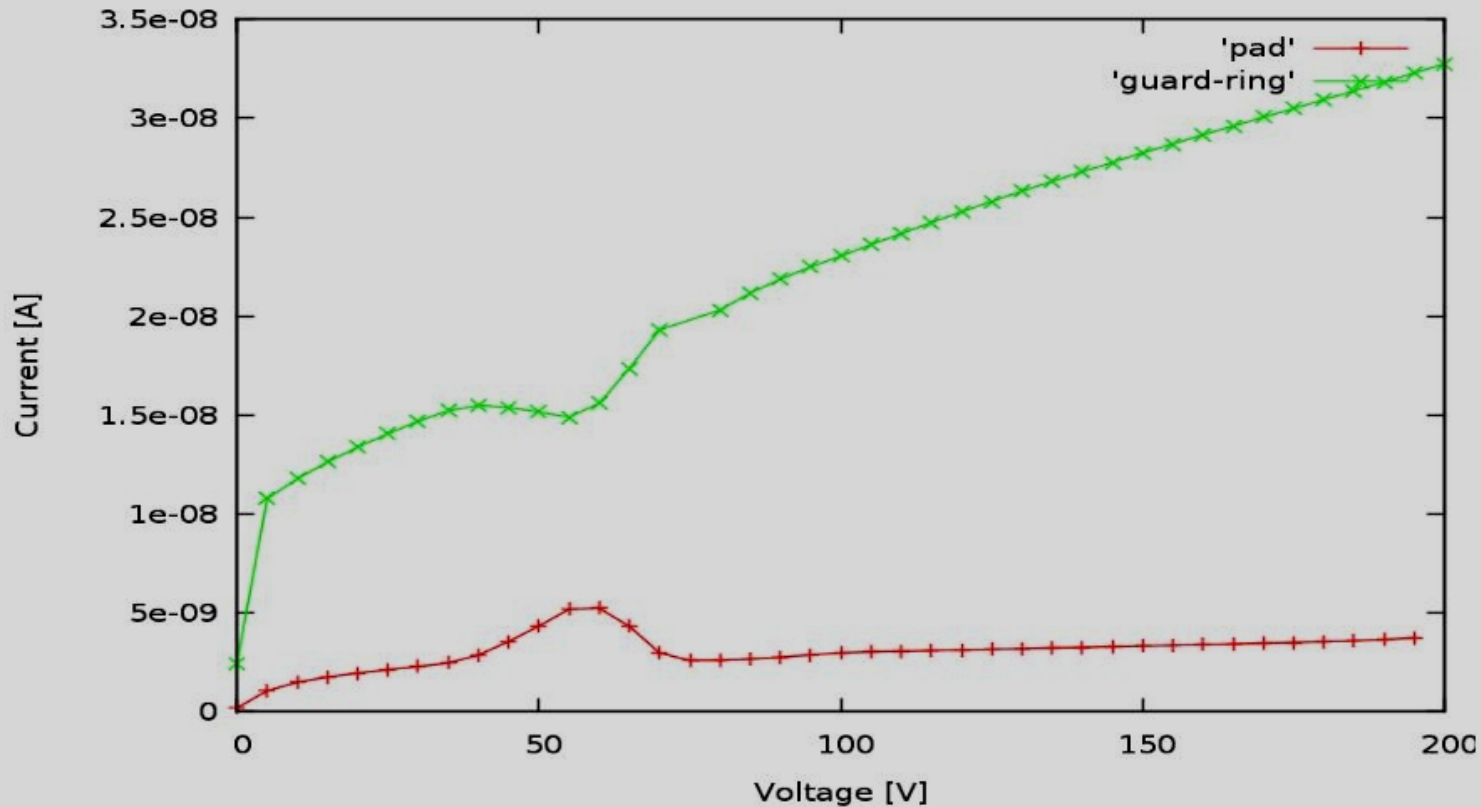
**Experimental data in figure were taken from measurement on pad L263 of detector 25**

Here: **A** - geometrical/material factor,  **$\psi$**  - diffusion potential = 0.7 V,  
**N** - donor concentration in Si bulk, **U, C** - voltage, capacitance

From the slope of linear fit in figure one can roughly estimate value of  **$N \sim 7 \cdot 10^{11}$  [1/cm<sup>3</sup>]**,  
and hence silicon resistivity to be about **6 – 8 k $\Omega$ cm**.

Value of depletion voltage can be also roughly estimated from figure to be in range 30 – 60V.

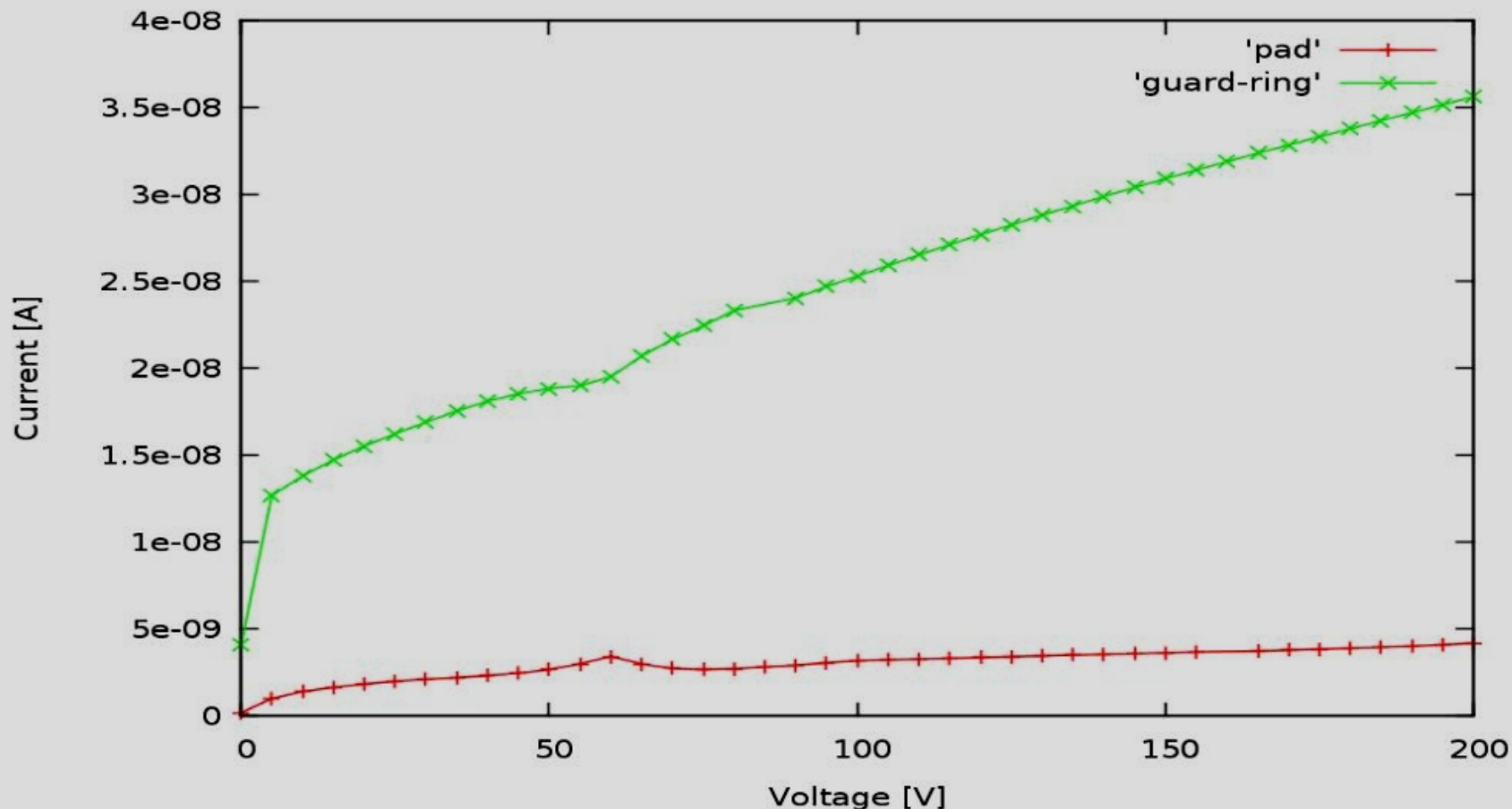
# Pad + GR measurements: current – voltage characteristics



## I – V measurement on detector 25.

The voltages on pad 64L2 and most inner guard-ring were applied simultaneously. One can see that in region 40 – 70V, current division between pad and guard ring is disturbed. It is result of specific geometry of electric field in boundary region – **pad 64L2 has relatively long „common boundary” with guard ring – about 28 mm!** That is why the effect is clearly visible. **Next slide presents pad 63L2 with „common boundary” of about 2 mm – the effect is not so strong.**

# Pad + GR measurements - current – voltage characteristics



## I – V measurement on detector 25

The voltages on **pad 63L2** and most inner guard-ring were applied simultaneously. As was mentioned in previous slide, the effect of „common boundary” is not so strongly visible. It is worth to mention that measured values of currents were slightly smaller than values reported in Hamamatsu data sheet.

# Conclusions

- The sensors measurements were done on two of twenty supplied by Hamamatsu detectors  
All the measured values were within specification
- C-V measurements indicate that Si material used by Hamamatsu has very high resistivity, what resulted in relatively low value of depletion voltage
- Low values of currents in I –V test measurements prove that minority carriers lifetime in Si is long (over 1 ms), what confirms high quality of Si material used by H-u company
- The visual inspection show good uniformity of current values from pad to pad, non degraded value of minority carriers lifetime and small values of pad currents at  $U > 3 U_{\text{depletion}}$ . This again confirm an excellent technological process used by Hamamatsu
- Obtained results and good reputation of H-u company allow believe that non-investigated detectors are also the same high quality
- Next step : used this detectors together with FE electronics in beam tests at DESY

More transparencies



# Possible explanation of common boundary effect (1)

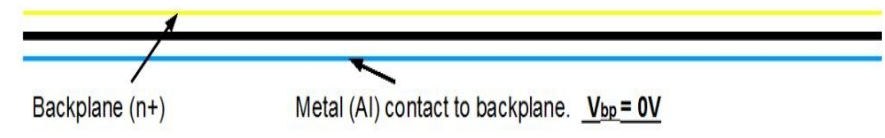
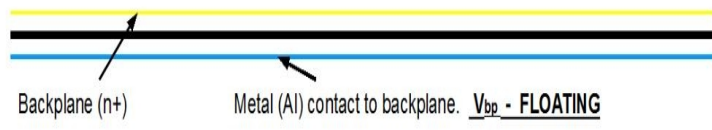
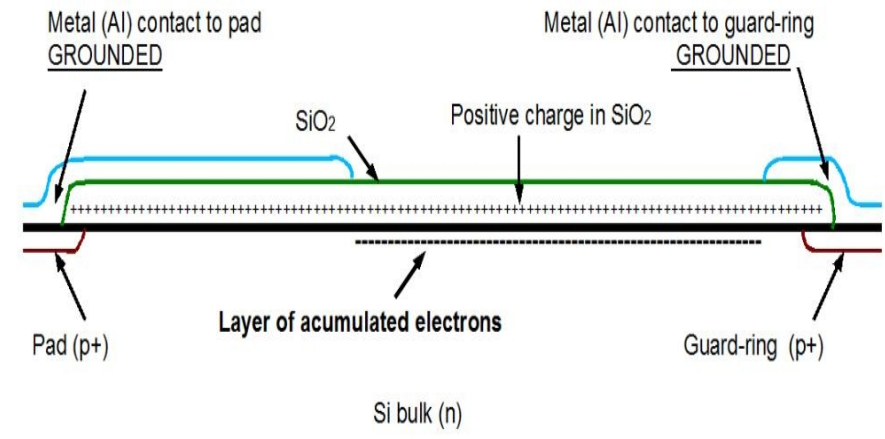
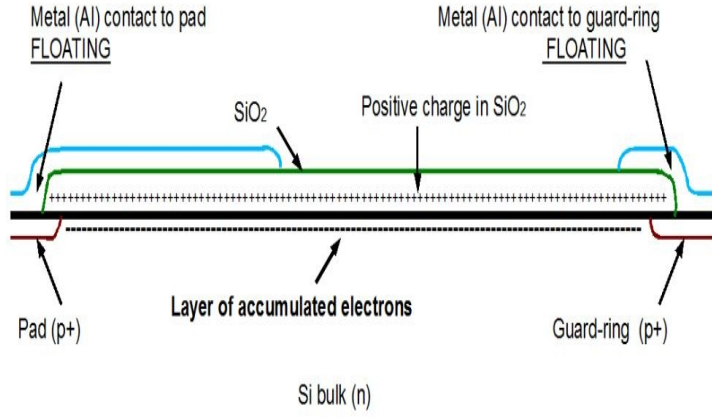


Figure 1.

Figure 2

# Possible explanation of common boundary effect (2)

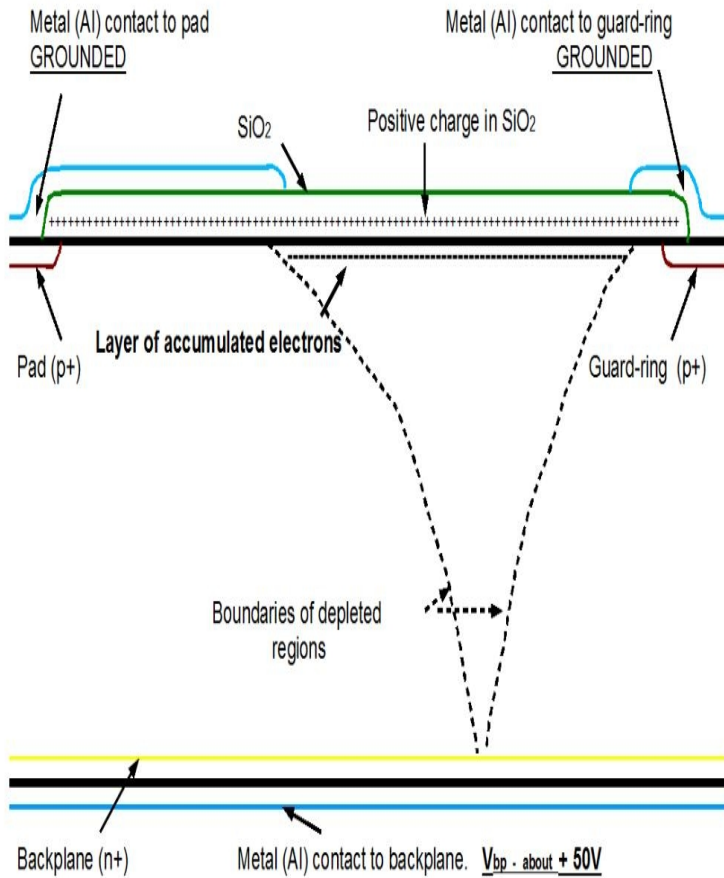


Figure 3

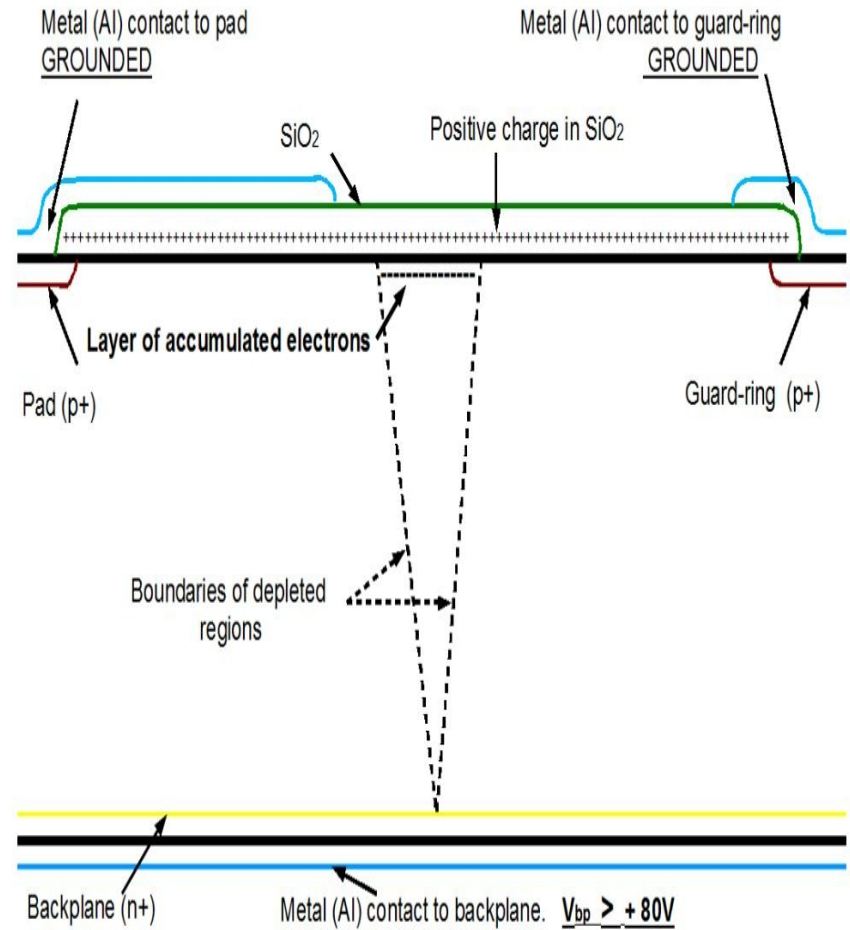


Figure 4